Hydroboration of carbon–tungsten triple bonds: crystal structures of the η^3-benzyl complexes $(\eta\text{-}C_5H_5)(CO)_2W\{\eta^3\text{-}CH[B(C_2H_5)_2]C_6H_4Me\text{-}4\}$ and $(\eta\text{-}C_5Me_5)(CO)_2W\{\eta^3\text{-}CH[B(C_2H_5)_2]C_6H_4Me\text{-}4\}$

Hubert Wadepohl [a], Gregory P. Elliott [b], Hans Pritzkow [a], F. Gordon A. Stone [b,c] and Andreas Wolf [a]

[a] *Anorganisch-Chemisches Institut der Universität, Im Neuenheimer Feld 270, D-69120 Heidelberg (Germany)*
[b] *School of Chemistry, University of Bristol, Bristol BS8 1TS (UK)*
[c] *Department of Chemistry, Baylor University, Waco, TX 76798-7348 (USA)*

(Received February 14, 1994)

Abstract

The Fischer carbyne complexes $[(\eta\text{-}C_5R_5)(CO)_2WC(p\text{-tolyl})]$ (R = H (**1c**)) (R = Me (**2c**)) react with $H_2B_2Et_4$ to afford the boryl substituted η^3-benzyl complexes $[(\eta\text{-}C_5R_5)(CO)_2W(\alpha,1,2\text{-}\eta^3\text{-}\{\alpha\text{-}BEt_2\}(p\text{-methyl})benzyl)]$ (R = H (**5b**)) (R = Me (**6b**)). On a column of silica, **5b** is slowly converted to the η^3-benzyl complex $[(\eta\text{-}C_5H_5)(CO)_2W(\alpha,1,2\text{-}\eta^3\text{-}\{(p\text{-methyl})benzyl\})]$ (**7**). Complex **5b** crystallizes in the monoclinic space group $P2_1/n$ with $a = 8.930(4)$, $b = 14.490(8)$, $c = 14.022(7)$ Å, $\beta = 98.70°$ and $Z = 4$. The structure was refined to $R = 0.026$ using 2649 unique observed diffractometer data. Complex **6b** crystallizes in the monoclinic space group $P2_1/a$ with $a = 16.124(3)$, $b = 8.728(2)$, $c = 18.190(3)$ Å, $\beta = 114.56(1)°$ and $Z = 4$. The structure was refined to $R = 0.033$ using 2064 unique observed diffractometer data. The gross structures of the two complexes are very similar, with $\alpha\text{-}BEt_2$-(*p*-methyl)benzyl ligands bound in an $\alpha,1,2\text{-}\eta^3$-enylic fashion to the tungsten atoms. In **6b**, one of the ethyl substituents is disordered. In both derivatives there is a weak attractive interaction between the boron atom of the boryl group and the carbon atom of one of the carbonyl ligands. In solution, **5b** exists as a mixture of two isomers. Extended Hückel (EH) and Fenske–Hall (FH) self-consistent field (SCF) molecular orbital (MO) calculations were conducted on several model complexes, $[(\eta\text{-}C_5H_5)(CO)_2W(\alpha,1,2\text{-}\eta^3\text{-benzyl})]$ (**9**), $[(\eta\text{-}C_5H_5)(CO)_2W\{\alpha,1,2\text{-}\eta^3\text{-}(anti\text{-}1\text{-}BH_2)allyl\}]$ (**10**) and $[(\eta\text{-}C_5H_5)(CO)_2W\{\alpha,1,2\text{-}\eta^3\text{-}(anti\text{-}\alpha\text{-}BH_2)benzyl\}]$ (**11**) as well as on **5b**. The bonding of the η^3-benzyl ligand to the metal was found to be similar in all cases and comparable with $[(\eta\text{-}C_5H_5)(CO)_2W(\alpha,1,2\text{-}\eta^3\text{-allyl})]$. Bonding overlap between empty π orbitals on the boryl group and two of the four π^* ligand group orbitals of the two CO molecules was found in **5b**.

Key words: Tungsten; Carbyne; Hydroboration; Structure

1. Introduction

The reactions of mononuclear transition metal alkylidyne (carbyne) complexes with the simplest electrophile — the proton — have been studied in some detail [1]. It is thought that the site of kinetic attack by the electrophile is the alkylidyne carbon, although the location of the proton in the final product may be quite different. Depending on the steric and electronic properties of the metal fragments the thermodynamic products can be alkylidyne hydrides or carbene complexes with or without agostic interactions or their follow-up products. These products correspond to location of the hydrogen atom on the metal atom, "over" the metal–carbon triple bond, or at the alkylidyne carbon atom respectively.

Borane (BH_3) and its organyl derivatives show a more complex reactivity, since the electrophilic attack is always accompanied or followed by hydride transfer from boron. The Fischer-type carbyne complexes $[(\eta\text{-}C_5R_5)(CO)_2WCR']$ (R = H; R' = Me, *p*-tolyl, or Ph) (**1**) (R = Me; R' = *p*-tolyl (**2**)) react with $BH_3 \cdot THF$ (THF ≡ tetrahydrofuran) to afford the ditungsten compounds $[(\eta\text{-}C_5R_5)(CO)_2W]_2[\mu\text{-}R'CB(H)CH_2R']$ (**3**, **4**) [2]. Compounds **3** and **4** are analogs of the well-known

Correspondence to: Priv. Doz. Dr. H. Wadepohl.

0022-328X/94/$7.00
SSDI 0022-328X(94)24657-5

μ-alkyne complexes $[(\eta\text{-}C_5R_5)(CO)_2M]_2(\mu\text{-}\eta^2\text{:}\eta^2\text{-}R'CCR')$ (M = Cr, Mo or W), the boron containing bridging ligand being isoelectronic with an alkyne.

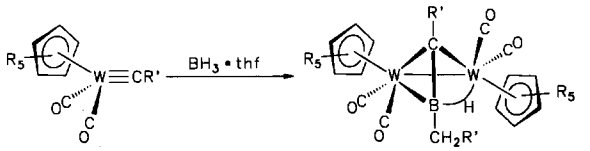

1, R = H, R' = Me, *p*-Tolyl, Ph
2, R = Me, R' = *p*-Tolyl

3, R = H
4, R = Me

In contrast, the dialkylborane-6 reagent 9-borabicyclo [3.3.1] nonane (9-BBN) affords stable products of type **5** with phenyl-substituted metal carbynes [2]. Both the boryl group and the hydride end up on the former carbyne carbon atom. The thus-formed boryl substituted benzyl ligand is η^3 bonded to the tungsten atom via the benzylic carbon atom and a carbon–carbon bond of the arene.

2. Results and discussion

2.1. Preparations, spectroscopy and structure analyses

The tetraalkyldiborane "Et_2BH" [3] reacts very readily with **1c** and **2c** to give the **5b** and **6b** respectively. The products can be isolated as orange–red crystals by recrystallization from non-polar hydrocarbon solvents. As expected for compounds with dialkylboryl groups, **5b** and **6b** are quite air sensitive. On a silica column, **5b** is slowly converted into the known [4] π-benzyl complex **7**. Obviously hydrolysis of **5b** is caused by residual water adsorbed on the surface of the "dry" silica.

X-ray structure analyses were carried out for **5b** and **6b**. Fractional atomic coordinates are given in Tables 1 and 2, and selected bond lengths and angles in Tables 3 and 4. The molecules are shown in Figs. 1 and 2. The general features of the structures of **5b** and **6b** are

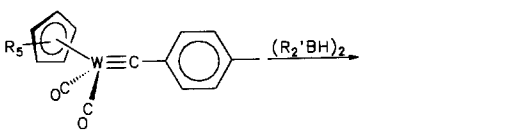

1c, R = H
2c, R = Me

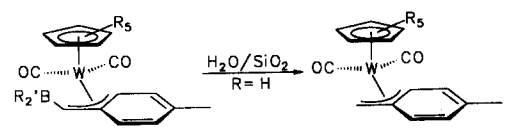

5a, R = H, R_2' = 9-BBN
5b, R = H, R' = Et
6b, R = Me, R' = Et

7, R = H

Formule 2

TABLE 1. Atomic coordinates and equivalent isotropic displacement parameters for **5b**, where U_{eq} is defined as one third of the trace of the orthogonalized U_{ij} tensor

	x (Å² × 10⁴)	*y* (Å² × 10⁴)	*z* (Å² × 10⁴)	U_{eq} (Å × 10³)
W(1)	1520(1)	1418(1)	2348(1)	45(1)
O(1)	495(5)	3342(3)	1560(3)	77(1)
O(2)	3904(5)	2713(3)	3514(3)	83(1)
B(1)	−1469(7)	2067(5)	2704(5)	57(2)
C(1)	288(5)	689(3)	3532(3)	44(1)
C(2)	1343(6)	1228(3)	4153(4)	46(1)
C(3)	2466(6)	808(4)	4832(4)	50(1)
C(4)	2535(6)	−124(4)	4937(4)	52(1)
C(5)	1508(7)	−668(4)	4326(4)	56(1)
C(6)	440(6)	−292(4)	3643(4)	53(1)
C(7)	−794(6)	1102(4)	2786(4)	50(1)
C(8)	3688(6)	−576(4)	5700(4)	70(2)
C(9)	−1390(8)	2781(4)	3569(5)	77(2)
C(10)	−1690(14)	3750(5)	3424(7)	148(4)
C(11)	−2708(6)	2275(4)	1780(5)	69(2)
C(12)	−2810(8)	1673(5)	898(5)	92(2)
C(13)	794(6)	2618(4)	1913(4)	56(1)
C(14)	3000(6)	2225(4)	3103(4)	57(1)
C(15)	3520(8)	631(5)	1838(5)	77(2)
C(16)	2438(10)	−43(5)	1925(5)	82(2)
C(17)	1153(9)	149(5)	1285(5)	87(2)
C(18)	1404(9)	958(5)	778(4)	80(2)
C(19)	2882(8)	1252(5)	1113(4)	72(2)

remarkably similar. However, the accuracy of the structure determination of **6b** is reduced owing to disorder of one of the ethyl groups of the BEt_2 moiety. The (α-boryl)*p*-methylbenzyl ligands are bonded in a π-enylic fashion to the tungsten atoms. As in **5a** the bonds from W(1) to the "inner" carbon atoms C(1) of the η^3-enyl system are about 0.2 Å longer than the bonds to the "outer" carbon atoms C(2) and C(7). Of the boron–carbon bonds the one to the metal-bound enylic carbon C(7) is the shortest. The C(7)(H)B group is twisted around C(1)–C(7) in a way that makes the boron atom farther from and the hydrogen closer to the tungsten atom. The torsion angle C(2)–C(1)–C(7)–B(1) is 25° in **5b** and 26° in **6b**.

The former arene rings show carbon–carbon bond length alternation consistent with some localization of double and single bonds. Averaged distances are 1.36 Å (**5b**), 1.35 Å (**6b**) for the "double bonds" C(3)–C(4), C(5)–C(6) and 1.41 Å (**5b**), 1.42 Å (**6b**) for the "single bonds" C(1)–C(6), C(2)–C(3) and C(4)–C(5). The *p*-methylbenzyl residues are nearly planar; deviations from the best planes through C(1)–C(8) are 0.02 Å (**5b**) and 0.06 Å (**6b**).

Interesting comparisons may be made with the structures of other complexes which have an η^3-enyl unit bound to a $[(\eta\text{-}C_5H_5)(CO)_2M]$ (M = Mo or W) fragment [5–8]. Complexes of the type $[(\eta\text{-}C_5H_5)$

TABLE 2. Atomic coordinates and equivalent isotropic displacement parameters for **6b**, where U_{eq} is defined as one third of the trace of the orthogonalized U_{ij} tensor.

	x (Å×10⁴)	y (Å×10⁴)	z (Å×10⁴)	U_{eq} (Å×10³)
W(1)	2976(1)	49(1)	2651(1)	54(1)
C(1)	3704(6)	−1739(12)	2129(5)	62(2)
C(2)	4490(6)	−913(12)	2692(6)	65(2)
C(3)	5121(6)	−1712(13)	3369(6)	72(3)
C(4)	5042(7)	−3207(14)	3513(6)	78(3)
C(5)	4306(7)	−4035(12)	2933(7)	78(3)
C(6)	3671(7)	−3317(11)	2304(6)	70(3)
C(7)	2978(7)	−950(14)	1486(6)	70(3)
C(8)	5730(8)	−4002(14)	4269(7)	107(4)
B(1)	2959(11)	514(17)	1037(8)	97(5)
C(9)	3848(10)	1423(17)	1093(8)	128(7)
C(10)	4177(12)	928(20)	487(11)	173(7)
C(11A)	1943(30)	597(42)	320(22)	99(14)
C(12A)	1573(28)	2105(37)	19(22)	151(17)
C(11B)	2150(22)	1279(35)	312(24)	154(20)
C(12B)	1257(21)	587(30)	67(18)	120(12)
C(13)	2721(7)	2067(13)	2139(7)	80(3)
O(1)	2553(6)	3315(9)	1943(5)	110(3)
C(14)	3986(7)	1294(11)	3398(6)	73(3)
O(2)	4561(5)	2066(8)	3822(4)	98(2)
C(15)	2645(7)	−492(12)	3748(6)	71(3)
C(16)	2456(7)	−1874(11)	3322(6)	66(3)
C(17)	1736(7)	−1603(13)	2556(6)	70(3)
C(18)	1500(6)	−28(15)	2519(6)	81(3)
C(19)	2054(7)	664(13)	3276(7)	75(3)
C(20)	3332(8)	−360(14)	4633(6)	114(5)
C(21)	2803(8)	−3424(13)	3670(7)	104(4)
C(22)	1221(7)	−2728(14)	1897(6)	114(5)
C(23)	664(7)	796(16)	1877(7)	125(5)
C(24)	1949(10)	2240(13)	3554(8)	126(5)

TABLE 3. Selected bond lengths for **5b** and **6b** with estimated standard deviations in parentheses

	Bond length (Å)	
	5b	**6b**
W(1)–C(1)	2.374(5)	2.374(9)
W(1)–C(2)	2.573(5)	2.552(9)
W(1)–C(7)	2.290(5)	2.293(10)
C(1)–C(2)	1.417(7)	1.45(1)
C(1)–C(6)	1.434(7)	1.42(1)
C(1)–C(2)	1.442(7)	1.44(1)
C(2)–C(3)	1.413(7)	1.41(1)
C(3)–C(4)	1.358(8)	1.35(1)
C(4)–C(5)	1.400(8)	1.42(1)
C(5)–C(6)	1.360(8)	1.33(1)
B(1)–C(7)	1.521(9)	1.51(1)
B(1)–C(9)	1.586(9)	1.60(2)
B(1)–C(11)	1.600(8)	[a]
W(1)–C(13)	1.922(6)	1.96(1)
W(1)–C(14)	1.952(6)	1.96(1)
C(13)–C(1)	1.174(6)	1.14(1)
C(14)–C(2)	1.159(6)	1.15(1)
W(1)–C(15)...C(19)	2.275(6)...2.377(6)	2.28(1)...2.42(1)

[a] Owing to disorder the value cannot be determined precisely.

TABLE 4. Selected bond angles for **5b** and **6b** with estimated standard deviations in parentheses

	Bond angle (°)	
	5b	**6b**
C(2)–C(1)–C(6)	115.9(5)	115.4(9)
C(2)–C(1)–C(7)	121.8(5)	120.9(9)
C(1)–C(2)–C(3)	121.0(5)	118.2(9)
C(2)–C(3)–C(4)	121.2(5)	124.8(10)
C(3)–C(4)–C(5)	118.7(5)	117.8(10)
C(4)–C(5)–C(6)	122.0(5)	120.5(10)
C(1)–C(6)–C(5)	121.2(5)	124.2(10)
C(1)–C(7)–C(8)	130.7(5)	132.1(10)
C(7)–B(1)–C(9)	124.8(5)	124.6(12)
C(7)–B(1)–C(11)	116.9(6)	[a]
C(9)–B(1)–C(11)	116.2(5)	[a]
W(1)–C(13)–C(1)	170.6(5)	169.5(11)
W(1)–C(14)–C(2)	176.9(5)	177.7(9)
B(1)...C(13)	2.575	2.39

[a] Owing to disorder the value cannot be determined precisely.

$(CO)_2M(\eta^3\text{-allyl})]$ (M = Mo or W) can exist in two different conformations **A** and **B** which differ in the orientation of the allyl ligand with respect to the C_5H_5 ring. In solution, the *exo* (**A**) and *endo* (**B**) conformers are in equilibrium with one another [5]. In the crystalline state, only the *exo* conformers were found for $[(\eta\text{-}C_5H_5)(CO)_2Mo(\eta^3\text{-allyl})]$ [6a] and $[(\eta\text{-}C_5H_5)(CO)_2Mo(\eta^3\text{-cyclohexenyl})]$ [6b]. In contrast, an *endo* orientation of the η^3-enyl substructures is attained in crystalline $[(\eta\text{-}C_5H_5)(CO)_2M\{\alpha,1,2\text{-}\eta^3\text{-}(p\text{-methyl})\text{benzyl}\}]$ (M = Mo [7] or W [9]). These two complexes show only two CO stretches in solution [4], which rules out an *exo–endo* equilibrium.

As can be seen from Figs. 1 and 2, *exo*-like orientations of the *p*-methylbenzyl ligands are adopted in crystalline **5b** and **6b**. However, the η^3-enyl units are rotated by about 17° about the axis W–(η^3-enyl) in

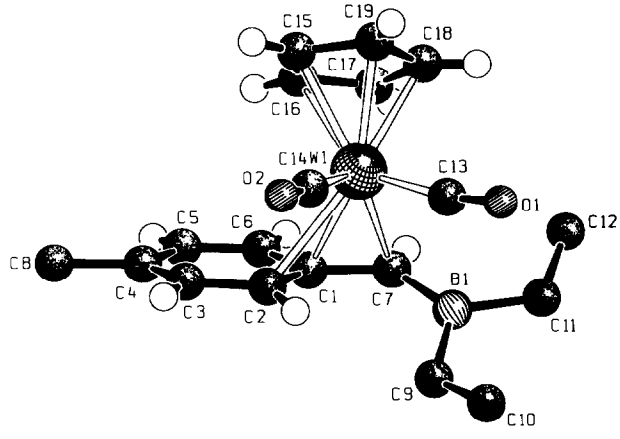

Fig. 1. Molecular structure of **5b**. The methyl and methylene hydrogen atoms are omitted for clarity.

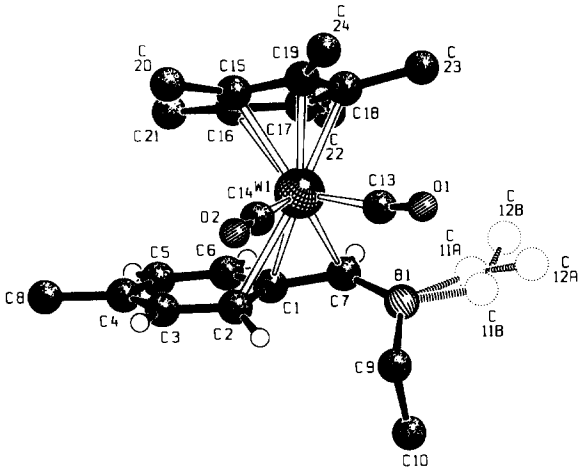

Fig. 2. Molecular structure of **6b**. The methyl and methylene hydrogen atoms are omitted for clarity.

such a way that the *p*-tolyl group is moved away from the C_5H_5 ligand.

In both derivatives **5b** and **6b** there appears to be a weak attractive interaction between the boryl group and the C(13) atom of one of the carbonyl ligands. Although the distances B(1)–C(13) (2.575 Å in **5b**; 2.39 Å in **6b**) cannot be considered as bonding, the donor–acceptor interactions are apparent from the bending of the participating CO ligands and from the pyramidalization at B(1), which is displaced from the plane defined by C(7), C(9) and C(11) in the direction of C(13).

The ^1H and ^{13}C NMR spectra of **5b** and **6b** show the signal patterns characteristic of substituted η^3-benzyl complexes (Tables 5 and 6). Unlike the η^3-benzyl complexes $[(\eta\text{-}C_5R_5)(CO)_2M(\eta^3\text{-}CH_2C_6H_4R')]$ (M = Mo [4,10] or W [4]), **5** and **6** are rigid on the NMR time scale at room temperature. The room-temperature NMR spectra of **5b** show two sets of signals because of the presence of two isomers. In a solution of **6b** only one isomer can be observed by NMR spectroscopy. This is also reflected by the IR spectra. Thus four bands at 1946.5(s), 1864.1(s), 1952.5(m) and 1882.9(m) cm^{-1} are observed in the ν_{CO} region for **5b** (in *n*-pentane) while **6b** shows only two CO stretches at 1932.9(s) and 1846.0(s) cm^{-1} (in *n*-hexane). Consistent with these observations, **5b** shows a shoulder (δ = 53.2) at the low field side of the broad ^{11}B resonance at δ = 42.6 while there is only one ^{11}B signal (δ = 51.6) for **6b**. The ^{11}B chemical shifts are at somewhat higher field than expected [11] for alkenylboranes.

In crystalline **5b**, only one isomer was found by X-ray crystallography (*vide supra*). This does not rule out an equilibrium of two isomers in solution. Therefore a crystalline sample of **5b** was dissolved in THF-d_8 at −100°C in an NMR tube and the cold solution transferred to the NMR probe pre-cooled to −80°C. At this temperature, only the ^1H NMR signals labelled with a superscript b in Table 5 were detected. Upon warming to −70°C, a second set of resonances appeared. The final intensity ratio of the two sets was 5:1 at room temperature and this feature did not change significantly when the sample was recooled to −80°C. As suggested earlier [2], the two isomers probably differ according to whether the tungsten is ligated by C(7), C(1) and C(2), as found in the crystal (*anti* position of the boryl substituent), or by C(7), C(1) and C(6) (*syn* position of the boryl substituent). Alterna-

TABLE 5. ^1H NMR data (200.1 MHz) for **5b** (in THF-d_8) and **6b** (in C_6D_6)

	δ						
	C_5R_5	C_2H_5	*p*-CH_3	H(7)	H(2)	H(3)	H(5), H(6) [a]
5b [b]	5.03 (s)	0.82 (m, br)	2.26 (s)	3.98 (s)	4.96 (dd, J_{HH} = 7.1, 1.5 Hz)	7.09 (dd, J_{HH} = 7.1, 1.5 Hz)	6.97 (dd, J_{HH} = 8.6, 1.5 Hz), 7.22 (dd, J_{HH} = 8.6, 1.5 Hz)
5b [c]	5.44 (s)	0.91 (m, br)	2.21 (s)	4.26 (s)	5.62 (d, J_{HH} = 6.6 Hz)	6.62 (d, J_{HH} = 6.4 Hz)	6.70 (d, J_{HH} = 6.8 Hz), 7.15 (d, J_{HH} = 6.8 Hz)
6b	1.41 (s)	1.30 (m, br)	1.96 (s)	2.74 (s)	5.49 (d, J_{HH} = 6.0 Hz)	6.61 (d, J_{HH} = 6.0 Hz)	6.27 (d, J_{HH} = 8.0 Hz), 6.76 (d, J_{HH} = 8.0 Hz)

[a] Assignment to H(5) or H(6) arbitrary.
[b] Major isomer, see text.
[c] Minor isomer.

TABLE 6. ^{13}C NMR data (50.3 MHz) for **5b**

δ (THF-d_8, −80°C)
240.2 (CO); 229.5 (CO); 136.6, 134.7, 132.0, 131.4 (C(3)–C(6)); 101.9 (C(2)); 92.2 (C_5H_5); 84.8 (C(1)); 48.1 (C(7)); 21.5 (*p*-CH_3); 17.0 (br), 15.1 (br) (B–CH_2); 12.2, 10.4 (B–CH_2–CH_3)

tively, there could be *exo* and *endo* orientation of the *p*-methylbenzyl ligand.

In the low temperature (−80°C) ^{13}C NMR spectrum of the sample of **5b**, which was made up below −90°C, two sets of resonances were observed for the two ethyl groups of the boryl substituent (Table 6). This inequivalence of the ethyl groups must be caused by a hindrance of rotation around the B–C(7) bond and is an indication of some double-bond character.

2.2. *Molecular orbital calculations*

Molecular orbital calculations were carried out (i) to gain insight into the preference for *exo*- or *endo*-like orientation of the benzyl ligands in complexes such as **5–7** and (ii) to establish the nature of the interaction of the η^3-(α-boryl)enyl-type ligands with the $[(\eta\text{-}C_5H_5)(CO)_2W]$ fragment. Both the shortening of the $B\text{–}C_{enyl}$ bond and the interaction of the boron atom with a carbonyl carbon atom are interesting features of **5** and **6** which have no precedent in the literature.

The electronic structure of the complexes $[(\eta\text{-}C_5H_5)LL'Mo(\eta^3\text{-allyl})]$ (**8**) has been studied in some detail by Hoffmann's group [12] using the extended Hückel technique. We conducted EH calculations for three model complexes $[(\eta\text{-}C_5H_5)(CO)_2W(\alpha,1,2\text{-}\eta^3\text{-benzyl})]$ (**9**), $[(\eta\text{-}C_5H_5)(CO)_2W\{\alpha,1,2\text{-}\eta^3\text{-}(anti\text{-}1\text{-}BH_2)\text{allyl}\}]$ (**10**) and $[(\eta\text{-}C_5H_5)(CO)_2W\{\alpha,1,2\text{-}\eta^3\text{-}(anti\text{-}\alpha\text{-}BH_2)\text{benzyl}\}]$ (**11**). In all cases idealized geometries were assumed with the planar η^3-bound ligands parallel to the plane of the carbonyl groups. A fragment molecular orbital approach was used. The molecules were partitioned into the two closed-shell moieties $[(\eta\text{-}C_5H_5)(CO)_2W]^-$ and $[\eta^3\text{-ligand}]^+$.

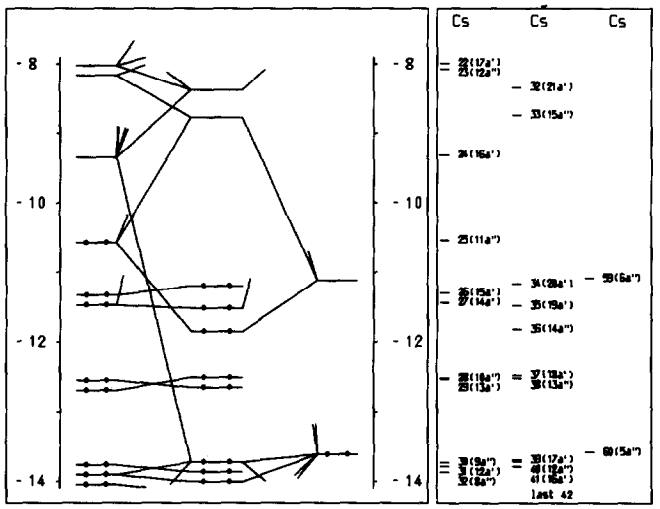

Fig. 3. Orbital correlation diagram for $[(\eta\text{-}C_5H_5)(CO)_2W(\eta^3\text{-allyl})]$: left, $[(\eta\text{-}C_5H_5)(CO)_2W]^-$; right, $allyl^+$.

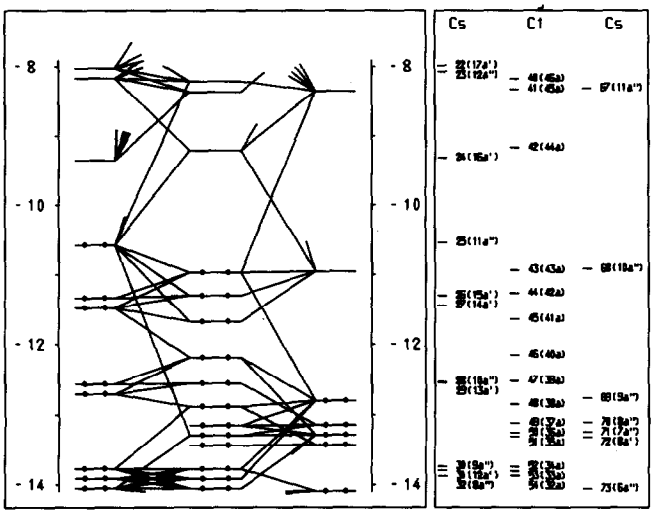

Fig. 4. Orbital correlation diagram for **9**: left, $[(\eta\text{-}C_5H_5)(CO)_2W]^-$; right, $benzyl^+$.

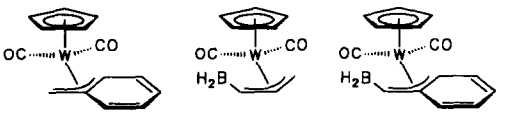

9 **10** **11**

The frontier orbitals of the $[(\eta\text{-}C_5H_5)(CO)_2W]$ fragment are well known [13] and need not be reiterated here. Their interactions with the frontier orbitals of the η^3-enyl ligands in the *exo* orientation are given in Figs. 3–6. The general features of the orbital interaction diagrams for **8** and **9–11** are quite similiar. In all cases there is not much difference between the *exo* and *endo* orientations of the η^3-enyl units.

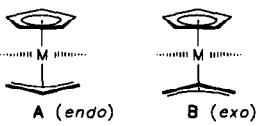

This is because the main interaction is between the $[(\eta\text{-}C_5H_5)(CO)_2W]$ fragment orbital 11a″ (mainly W d_{xz}, filled for $[(\eta\text{-}C_5H_5)(CO)_2W]^-$) and the lowest unoccupied molecular orbitals (LUMOs) of the cationic η^3-enyl ligands (Fig. 7) which have small (or zero [14*]) linear-combination-of-atomic-orbitals coefficients at the central carbon atoms. Despite extensive mixing of orbitals due to the absence of symmetry, this situation essentially persists over the whole series **9–11**. The LUMOs of $[1\text{-}BH_2\text{–allyl}]^+$ and $[\alpha\text{-}BH_2\text{–benzyl}]^+$ are strongly B–C π bonding. On complex formation with the metal-containing fragments, these orbitals become populated resulting in a partial boron–carbon double

* A reference number with an asterisk indicates a note in the list of references.

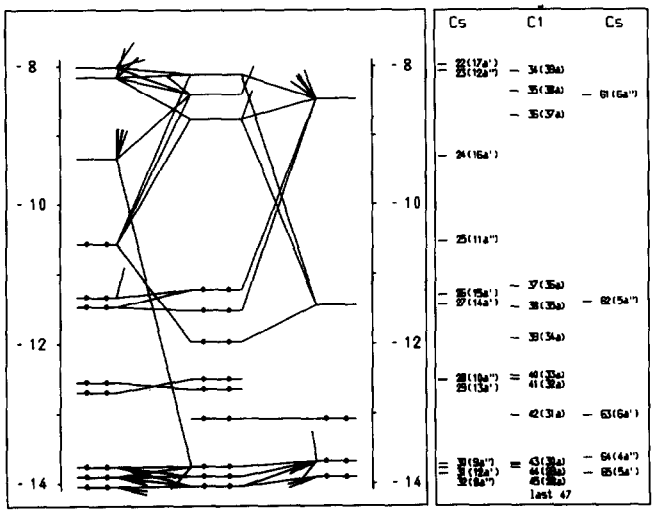

Fig. 5. Orbital correlation diagram for **10**: left, $[(\eta\text{-}C_5H_5)(CO)_2W]^-$; right, $[(anti\text{-}1\text{-}BH_2)allyl)]^+$.

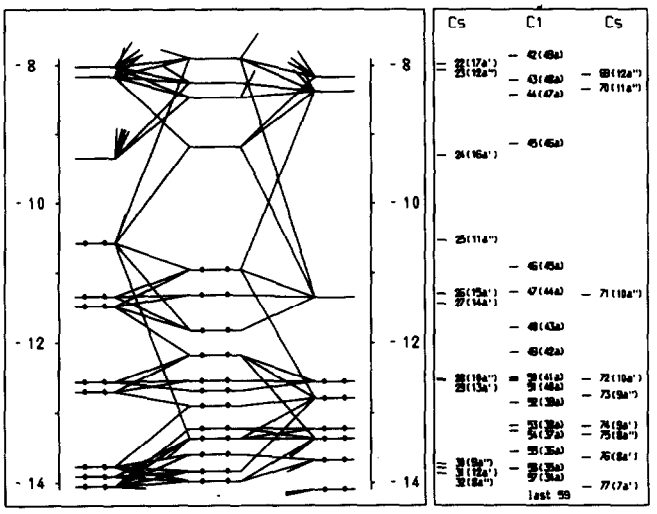

Fig. 6. Orbital correlation diagram for **11**: left, $[(\eta\text{-}C_5H_5)(CO)_2W]^-$; right, $[(anti\text{-}\alpha\text{-}BH_2)benzyl)]^+$.

bond. This can be clearly seen in the structures of **5b** and **6b**, where the distances B(1)–C(7) are considerably shortened (1.521(9) and 1.51(1) Å). It also explains the observed high field ^{11}B NMR chemical shift [15] and the considerable barrier to rotation around the B(1)–C(7) bond.

In **9** and **11** the tendency for bond length alternation within the benzyl ring is apparent from the variation in carbon–carbon overlap populations.

EH and Fenske-Hall MO calculations were also carried out using the experimental geometry found for **5b**. As expected from the different calculational methods the numerical results of the two calculations differ. The ordering of the frontier orbitals and their composition are, however, comparable. The composition of the frontier molecular orbitals of **5b**, as obtained from the FH calculation, is summarized in Table 7.

There is some orbital overlap between the boron atom and the carbonyl ligand nearest to it. The total Mulliken overlap population between B and the carbon atom of this CO group is positive (0.081 (EH); 0.082 (FH)), indicating a weakly bonding interaction. Because of the lack of symmetry this interaction is difficult to track down. It appears to be localized mainly in two orbitals, the highest occupied molecular orbital (HOMO) and the second-highest occupied molecular orbital (HOMO-2). The HOMO of **5b** is mainly derived from the 15a′ fragment orbital of $[(\eta\text{-}C_5H_5)(CO)_2W]$ (90% (EH) and 92% (FH)) with a small contribution of an empty π orbital of the organoboron ligand. The HOMO-2 is the bonding combination of the $[(\eta\text{-}C_5H_5)(CO)_2W]$ 11*a*″ fragment orbital (the HOMO for $[\{\eta\text{-}C_5H_5\}\{CO\}_2W]^-$) and the LUMO of the α-borylbenzyl ligand. In a more localized view, there is bonding overlap between empty π orbitals on the boryl group and two of the four π^* ligand group orbitals of the two CO molecules (the FH interfragment overlap populations are 0.027 and 0.022 for the two relevant combinations). Although the latter orbitals are empty without the presence of a metal, they become populated in the complex by back donation from occupied metal π orbitals. Some electron density is transferred from a carbonyl carbon to the boron atom but is replenished at the carbon by increased back donation

TABLE 7. Energies and percentage compositions of important molecular orbitals in **5b**

ϵ (eV)	Composition (%)							
	W	2CO		C(1)	C(2)	C(7)	B	
		5σ [a]	2π [b]				Total	π
−3.48 (LUMO)	29	1	18	0	1	6	1	1
−8.88 (HOMO)	58	0	30	0	1	0	3	3
−9.96	56	0	29	1	0	1	1	1
−11.80	20	1	3	4	6	26	9	7
−13.16	1	0	0	4	1	3	26	0

[a] The two orbitals derived from the HOMO (5σ) of CO.
[b] The four orbitals derived from the LUMO (2π) of CO.

from the tungsten atom. This slightly increases the metal carbon bond strength for the CO ligand involved in this interaction, as can be seen from the metal CO–carbon overlap populations (0.945 compared with 0.884 (EH)).

In the literature there are several examples of donor acceptor interactions between carbonyl ligands and tricoordinated boryl compounds [16]. However, intermolecular interaction always takes place between the Lewis acidic boryl group and the oxygen atom of CO, which is of course much more basic than the metal-coordinated carbon atom. In the specific geometric arrangement found for crystalline **5** and **6** an intramolecular B · · · O interaction is clearly prohibited.

3. Experimental section

3.1. General procedures

All operations were carried out under an atmosphere of purified nitrogen (BASF R3-11 catalyst) using Schlenk techniques. Solvents were dried by conventional methods. The compounds $[(\eta\text{-}C_5R_5)(CO)_2W(CC_6H_4Me\text{-}4)]$ (R = H (**1**) [17]; R = Me (**2**) [18]) and tetraethyldiborane-6 [19] were prepared as described in the literature. NMR spectra were obtained on a Bruker AC 200 instrument (200.1 MHz for ^1H; 50.3 MHz for ^{13}C). Elemental analyses were performed by Mikroanalytisches Labor Beller, Göttingen.

3.2. Reaction of $[(\eta\text{-}C_5H_5)(CO)_2W(CC_6H_4Me\text{-}4)]$ (1) with tetraethyldiborane-6

Tetraethyldiborane-6 (0.4 ml, 2.85 mmol) was added to a THF solution (40 ml) of 1.2 g (2.9 mmol) of **1** at −20°C. The mixture was stirred at −20°C for about 1 h and then slowly warmed to room temperature. The solvent was removed from the dark-red solution under reduced pressure, and the residue was recrystallized from pentane (about 100 ml) at −20°C to give dark-red crystals of $[(\eta\text{-}C_5H_5)(CO)_2W(\eta^3\text{-}CH(BEt_2)C_6H_4Me\text{-}4)]$ (**5b**) (770 mg; 55%). Anal. Found: C, 47.95; H, 4.93. $C_{19}H_{23}BO_2W$ (478.04) calc.; C, 47.74; H, 4.85%.

When **5b** was chromatographed on a silica column (22 × 3 cm) with petrol–toluene (3:1), a dark-orange band developed. Without clear separation, the eluate turned from orange to red after about two thirds of the band was eluted. The red eluate was identified by IR spectroscopy as **5b**. The first orange fraction showed IR bands at 1950 and 1867 cm^{-1} together with additional bands due to **5b**. Solvent was removed *in vacuo* from this fraction and the residue was recrystallized from petrol at −20°C. The microcrystalline precipitate was washed with cold petrol and then redissolved in

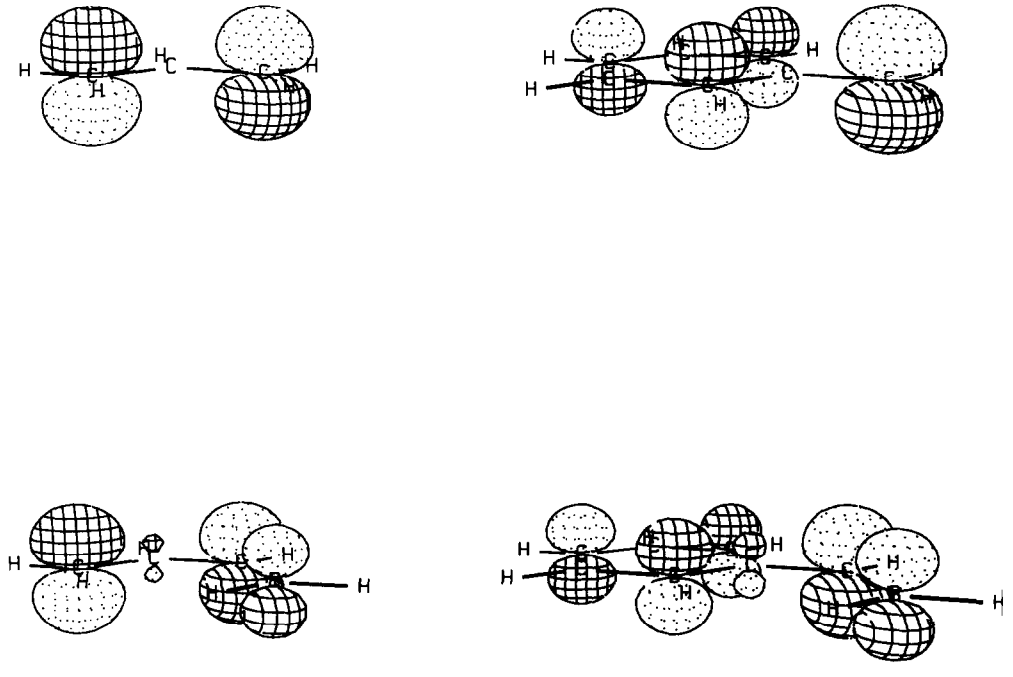

Fig. 7. Graphical representation of the LUMO of allyl$^+$ (top left), benzyl$^+$ (top right), [(*anti*-1-BH_2)allyl)]$^+$ (bottom left) and [(*anti*-α-BH_2)-benzyl]$^+$ (bottom right).

the same solvent. Upon cooling to −20°C, orange crystals of pure **7** precipitated.

3.3. Reaction of $[(\eta\text{-}C_5Me_5)(CO)_2W(CC_6H_4Me\text{-}4)]$ (1) with tetraethyldiborane-6

Tetraethyldiborane-6 (0.2 ml, 1.4 mmol) was added to a THF solution (40 ml) of 640 mg (0.75 mmol) (**2**) at −50°C. The orange solution turned red when it was slowly warmed to room temperature. After standing at room temperature over night, solvent was removed under reduced pressure. The dry residue was redissolved in petrol and filtered from a small amount of yellowish precipitate. Cooling to −20°C afforded $[(\eta\text{-}C_5Me_5)(CO)_2W(\eta^3\text{-}CH(BEt_2)C_6H_4Me\text{-}4)]$ (**6b**) (390 mg; 53%) as deep-orange crystals. Anal. Found: C, 52.33; H, 6.06. $C_{24}H_{33}BO_2W$ (548.17) calc.; C, 52.58; H, 6.07%.

3.4. X-ray crystal structure determination of $[(\eta\text{-}C_5H_5)(CO)_2W\{\alpha,1,2\text{-}\eta^3\text{-}CH[B(C_2H_5)_2]C_6H_4Me\text{-}4\}]$ (5b) and $[(\eta\text{-}C_5Me_5)(CO)_2W\{\alpha,1,2\text{-}\eta^3\text{-}CH[B(C_2H_5)_2]C_6H_4Me\text{-}4\}]$ (6b)

Crystals were mounted in Lindemann capillary tubes and transferred to a Stoe Siemens four-circle diffractometer. Intensity data were collected at ambient temperature and corrected for Lorentz, polarization and absorption effects (Table 8). The structures were solved by the heavy-atom method and refined by full-matrix least-squares using all measured unique reflexions [20*]. All non-hydrogen atoms were given anisotropic thermal parameters.

Some of the hydrogen atoms were located from difference Fourier maps and refined with isotropic atomic displacement parameters (hydrogen atoms on C(2) and C(7) for **6b**; all hydrogen atoms on the *p*-methylbenzyl ring and on C(7) for **5b**). All other hydrogen atoms were input in calculated positions.

Apparent disorder of one of the ethyl groups in **6b** was treated with a twofold split-atom model (site occupation factors refined to 0.46 and 0.54 respectively). The bonds C(11)–C(12) and C(9)–C(10) were restrained to be the same length.

The calculations were performed using the programs SHELXS-86 and SHELXL-93 [22]. Scattering factors and anomalous dispersion factors were taken from ref. 23. Graphical representations were drawn with the SCHAKAL-88 program [24].

TABLE 8. Details of the crystal structure determinations of $[(\eta\text{-}C_5H_5)(CO)_2W\{\alpha,1,2\text{-}\eta^3\text{-}CH(BEt_2)C_6H_4Me\text{-}4\}]$ (**5b**) and $[(\eta\text{-}C_5Me_5)(CO)_2W\{\alpha,1,2\text{-}\eta^3\text{-}CH(BEt_2)C_6H_4Me\text{-}4\}]$ (**6b**)

	5b	**6b**
Formula	$C_{19}H_{23}BO_2W$	$C_{24}H_{33}BO_2W$
Crystal habit; colour	Box; orange	Box; red
Crystal size (mm)	0.4 × 0.4 × 0.5	0.3 × 0.4 × 0.4
Crystal system	Monoclinic	Monoclinic
Space group	$P2_1/n$	$P2_1/a$
a (Å)	8.930(4)	16.124(3)
b (Å)	14.490(8)	8.728(2)
c (Å)	14.022(7)	18.190(3)
β (°)	98.70(4)	114.56(1)
V (Å^3)	1793.5	2328.3
Z	4	4
M_r	478.04	548.17
d_c (g cm^{-1})	1.770	1.564
F_{000}	928	1088
μ(Mo Kα) (cm^{-1})	64.5	49.8
X-radiation, λ (Å)	Mo Kα, graphite monochromated;	0.71069
Data collection temperature	Ambient	
2Θ range (°)	3–50	3–50
hkl range	−10/10, 0/17, 0/16	−19/17, 0/10, 0/21
Number of reflections measured	3162	4161
Unique	3162	4036
Observed [$I < 2\sigma(I)$]	2649	2064
Absorption correction	Empirical	Numerical
Number of parameters refined	237	299
R (obs. reflexions only)	0.026	0.033
wR_2 ($w = 1/[\sigma^2(F) + (A.P)^2 + B.P]$, $P = \max(F_o^2, 0) + \frac{2}{3}F_c^2$)	0.061	0.098
A, B	0.0254, 1.56	0.0404, 1.68

3.5. Molecular orbital calculations

EH calculations were carried out with CACAO [25] using the wavefunctions supplied with the package. The weighted Wolfsberg–Helmholtz formula [26] was employed. The coordinate system used was identical with that used by Schilling *et al.* [13]. The model complexes **9–11** were kept pseudo-octahedral with the cyclopentadienyl-ligand occupying three coordination sites and with W–C(O) angles of 90°. The distance from the metal to the planes of the allyl, 1-BH_2-allyl and α-BH_2-benzyl ligands was kept at 1.90 Å. C–C bond distances were 1.40 Å in the η-C_5H_5 and 1.42 Å in the η^3-enyl ligands. For the carbonyl ligands, M–C(O) bonds were set to 1.95 Å and C–O bonds to 1.15 Å.

The iterative SCF FH procedure [27] employs the atomic basis functions and the molecular geometry as the only adjustable parameters. The Slater-type orbitals STO basis functions used in the FH calculations have been developed by the Fenske group using the numerical Xα atomic orbital program of Herman and Skilman [28] in conjunction with the Xα-to-Slater basis program of Bursten and Fenske [29]. Exponents of 6s and 6p atomic orbitals for tungsten were set to 2.4. A value of 1.20 was used for the hydrogen exponent. After convergence of the SCF calculation the atomic basis set was transformed into a basis set of fragments with chemical meaning. The (α-boryl)benzyl ligand was always treated as a positively charged fragment. Negative charges were assigned to the metal-containing fragments ([{η-C_5H_5}$(CO)_2$W] or [{η-C_5H_5}W]). Using the frozen-orbital approximation [30] the first three occupied and all virtual orbitals of C_5H_5 above the e″ level (D_{5h}) were filled with 2.0 and 0.0 electrons respectively and deleted from the basis set transformation.

References and notes

1 A. Mayr, *Comments Inorg. Chem., 10* (1990) 227, and references cited therein; H.P. Kim and R.J. Angelici, *Adv. Organomet. Chem., 27* (1987) 51, and references cited therein; M.A. Gallop and W.R. Roper, *Adv. Organomet. Chem., 25* (1986) 121, and references cited therein; S.A. Brew and F.G.A. Stone, *Adv. Organomet. Chem., 35* (1993) 135, and references cited therein.

2 G.A. Carriedo, G.P. Elliott, J.A.K. Howard, D.B. Lewis and F.G.A. Stone, *J. Chem. Soc. Chem. Commun.*, (1984) 1585; D. Barratt; S.J. Davies, G.P. Elliott, J.A.K. Howard, D.B. Lewis and F.G.A. Stone, *J. Organomet. Chem., 325* (1987) 185.

3 R. Köster, G. Griasnow, W. Larbig and P. Binger, *Justus Liebigs Ann. Chem., 672*, (1964) 1.

4 F.A. Cotton and T.J. Marks, *J. Am. Chem. Soc., 91* (1969) 1339.

5 (a) A. Davison and W.C. Rode, *Inorg. Chem., 6* (1967) 2124; (b) J.W. Faller and M.J. Incorvia, *Inorg. Chem., 7* (1968) 840.

6 (a) J.W. Faller, D.F. Chodosh and D. Katahira, *J. Organomet. Chem., 187* (1980) 227; (b) J.W. Faller, H.H. Murray, D.L. White and K.H. Chao, *Organometallics, 2* (1983) 400.

7 F.A. Cotton and M.D. LaPrade, *J. Am. Chem. Soc., 90* (1968) 5418.

8 J.C. Jeffery, A.L. Ratermann and F.G.A. Stone, *J. Organomet. Chem., 289* (1985) 367.

9 H. Wadepohl and H. Pritzkow, *Acta Crystallogr., Sect. C, 48* (1992) 160.

10 R.B. King and A. Fronzaglia, *J. Am. Chem. Soc., 88* (1966) 709.

11 H. Nöth and H. Wrackmeyer, in P. Diehl, E. Fluck and R. Kosfeld (eds.), *NMR Basic Principles and Progress*, Vol. 14, *Nuclear Magnetic Resonance Spectroscopy of Boron Compounds*, Springer, Berlin, 1978, Chapter 9.

12 B.E.R. Schilling, R. Hoffmann and J.W. Faller, *J. Am. Chem. Soc., 101* (1979) 592.

13 B.E.R. Schilling, R. Hoffmann and D.L. Lichtenberger, *J. Am. Chem. Soc., 101* (1979) 585.

14 The LUMOs of allyl$^+$ and benzyl$^+$ have nodes at the central carbon atom.

15 H. Nöth and H. Wrackmeyer, in P. Diehl, E. Fluck and R. Kosfeld (eds.), *NMR Basic Principles and Progress*, Vol. 14, *Nuclear Magnetic Resonance Spectroscopy of Boron Compounds*, Springer, Berlin, 1978, Chapter 4.2.3.

16 (a) F. Klanberg, W.B. Askew and L. Guggenberger, *Inorg. Chem., 7* (1968) 2265; (b) J.S. Kristoff and D.F. Shriver, *Inorg. Chem., 13* (1973) 499; (c) V. Bätzel, U. Müller and R. Allmann, *J. Organomet. Chem., 102* (1975) 109; (d) V. Bätzel, *Z. Naturforsch., 31b* (1976) 342; (e) A.K. Chipperfield, C.E. Housecroft and P.R. Raithby, *Organometallics, 9* (1990) 479.

17 E.O. Fischer, T.L. Lindner, G. Huttner, P. Friedrich, F.R. Kreißl and J.O. Besenhard, *Chem. Ber., 110* (1977) 3397.

18 E. Delgado, J. Hein, J.C. Jeffery, A.L. Ratermann and F.G.A. Stone, *J. Chem. Soc., Dalton Trans.*, (1987) 1191.

19 R. Köster, in R. Köster (ed.), *Methoden der organischen Chemie (Houben-Weyl)*, Vol. XIII/3a Thieme, Stuttgart, 1982, Chapter A_2II.

20 Further details of the crystal structure investigation may be obtained from the Fachinformationszentrum Karlsruhe, Gesellschaft für wissenschaftlich-technische Information mbH, D-7514 Eggenstein-Leopoldshafen 2 (FRG), on quoting the depository numbers CSD 380057 (**5b**), CSD 380058 (**6b**), the names of the authors and the journal citation.

21 G.M. Sheldrick, SHELXS-86, *Acta Crystallogr. Sect. A., 46* (1990) 467.

22 G.M. Sheldrick SHELXL-93; *A Program for the Refinement of Crystal Structures from Diffraction Data*, Universität Göttingen, Göttingen, 1993.

23 *International Tables for X-ray Crystallography*, Vol. IV, Kynoch, Birmingham, 1974, p. 149.

24 E. Keller, "SCHAKAL 88, *A* FORTRAN *Program for the Graphical Representation of Molecular and Crystallographic Models*", Universität Freiburg, Freiburg, 1988.

25 C. Mealli and D.M. Proserpio, *J. Chem. Educ., 67* (1990) 399.

26 J.H. Ammeter, H.B. Bürgi, J.C. Thibeault and R. Hoffmann, *J. Am. Chem. Soc., 101* (1978) 3686.

27 M.B. Hall and R.F. Fenske, *Inorg. Chem., 11* (1972) 768.

28 F. Herman and S. Skillman, *Atomic Structure Calculations*, Prentice-Hall, Englewood Cliffs, NJ, 1963.

29 B.E. Bursten and R.F. Fenske, *J. Chem. Phys., 67* (1977) 3138; B.E. Bursten, R.J. Jensen and R.F. Fenske, *J. Chem. Phys., 68* (1978) 3320.

30 D.L. Lichtenberger and R.F. Fenske, *J. Chem. Phys., 64* (1976) 4247.